



Sudan University of Sciences and Technology
College of Graduate Studies



**Characterization of Urinary Tract Stones in Kassala State
using Multi-detector Computed Tomography**

توصيف حصاوي الجهاز البولي في ولاية كسلا باستخدام الأشعة المقطعية المحوسبه متعدده الكواشف

A Thesis Submitted for Partial Fulfillment for the Requirement of (Msc) degree
in Diagnostic Radiologic Imaging

By:-

Hoyam Ishag Siddig

Supervisor:

Dr. Ahmed Mostafa Abukonna

2020

الآية

قال تعالى :

(وقل رب اغفر وارحم و أنت خير الراحمين)

صدق الله العظيم

سورة المؤمنون - الآية (118)

Dedication

To

ALLHOPEMAKERS

Acknowledgement

This research project would not have been possible without the support of many people. I wish to express my gratitude to the supervisor, **Dr. Ahmed Mostafa Abukonna** who was abundantly helpful and offered invaluable assistance, support and guidance.

Also Special thanks to my mother and my father and all my family. Not forgetting to my best friend who always been there.

Abstract

Non-contrast Computed tomography is a method for evaluating the stones of urinary system. Together with the measurement of the stone density and size, become an important way of assessing patients with suspected stones.

The aim of this study was to evaluate the urinary system stones in patients who came with indication suspected to have urinary stone(s). The study sample was consisted of 100 patients with flank pain and clearly suspected for KUB stone or other pathological problem. A CT KUB was conducted at Kassala state. By the CT KUB we found the majority (91%) of patients developed (1-2) stones, the most stones located at pelvis (42%), lower calyces (21%) or mid ureter (10%) on either right site (43%) or left site (40%), since most of patients developed mild (28%) or moderate (36%) of Hydronephrosis and mostly (80%) negative Hydro- ureter, and The most common stone type (according to CT number) cystine stones followed by struvite stones.

For stone diameters, the sample found that the stone density was (386-1594) Hounsfield unit (HU) with mean 946.49 ± 244.55 , (3-33.5) with mean 10.33 ± 6.73 X-size and (3-53.5) with mean 14.28 ± 9.48 Y-size. The results found that the stone site and its number are significantly associate with age (P-value < 0.05), while neither Hydronephrosis nor Hydroureter depend on stone site (P-value > 0.05).

المستخلص

التصوير المقطعي غير المتباين هو طريقة لتقييم حصوات الجهاز البولي. جنبا إلى جنب مع قياس كثافة وحجم الحصاوي تصبح وسيلة مهمة لتقييم المرضى الذين يشتبه في وجود حصوات لديهم. كان الهدف من هذه الدراسة هو تقييم حصوات الجهاز البولي لدى المرضى الذين جاءوا بدلالة يشتبه في إصابتهم بحصوات المسالك البولية. تكونت عينة الدراسة من 100 مريض يعانون من آلام في الخصرة ومن الواضح أن هناك اشتباه في وجود حصوة أو أي مشكلة مرضية أخرى. تم إجراء فحص الأشعة المقطعية المحوسبة للكلي و المسالك البولية في ولاية كسلا. من خلال الفحص وجد أن غالبية (91%) من المرضى لديهم (1-2) حصوة ، معظم الحصوات موجودة في الحوض (42%) ، الكأس الكلوي السفلي (21%) و وسط الحالب (10%) في أي من الموقع الأيمن (43%) أو الموقع الأيسر (40%) ، معظم المرضى أصيبوا بدرجة خفيفة (28%) أو معتدلة (36%) من موه الكلية ومعظمهم (80%) ليس لديهم تجمع للسوائل في الحالب ، ونوع الحصوات الأكثر شيوعا حصوات الستين تليها حصوات الاستروفيت.

بالنسبة لأقطار الحجر ، وجدت العينة أن كثافة الحجر كانت (1594-386) وحدة هاونسفيلد بمتوسط 244.55 ± 946.49 ، (3-33.5) بمتوسط 6.73 ± 10.33 في المحور العرضي و (3-53.5) بمتوسط 9.48 ± 28.14 في المحور الطولي. وجدت النتائج أن موقع الحجر وعدده يرتبطان بشكل كبير بالعمر (قيمة $P < 0.05$) ، بينما لا يعتمد موه الكلية على موقع الحجر ($P < 0.05$).

List of tables

Table	Page No
Table (4. 1) distribution of participant according to gender:	29
Table (4. 2) distribution of participant according to age:	30
Table (4. 3) distribution of participant according to No. stones:	31
Table (4. 4) distribution of participant according to stone site:	32
Table (4. 5) distribution of participant according to stone location:	33
Table (4. 6) distribution of participant according to status of Hydro-nephrosis:	34
Table (4. 7) distribution of participant according to status of Hydro-ureter:	35
Table (4.8) distribution of participant according to stone type	36
Table (4. 9) distribution of participant according to other findings:	37
Table (4. 10) Descriptive statistics for study variables:	38
Table (4. 11) Chi-Square tests for association stone site and age:	38
Table (4. 12) Chi-Square tests for association No. of stones and age:	39
Table (4. 13) Chi-Square tests for association stone site and Hydro-nephrosis:	40
Table (4.14) Chi-Square tests for association stone site and Hydro-ureter	41

List of Figures

Figure	Page No
Figure (2. 1) showed the internal structure of kidney's functional unit	4
Figure (2. 2) demonstrate the and blood pathway from and into the kidney	5
Figure (2. 3) showed the internal structure of kidney's functional unit	6
Figure (2. 4) demonstrate the and blood pathway from and into the kidney (Lauder et al., 2018)	7
Figure (2. 5) demonstrate the renal structure with its specific function (Crabbs and McDorman, 2018)	8
Figure (3. 1) CT scan machine show gantry and couch	26
Figure (4. 1) distribution of participant according to gender	29
Figure (4. 2) distribution of participant according to age	30
Figure (4. 3): distribution of participant according to No. of stones	31
Figure (4. 4) distribution of participant according to stone site	32
Figure (4. 5) distribution of participant according to stone location	33
Figure (4. 6) distribution of participant according to status of Hydro-nephrosis	35
Figure (4. 7) distribution of participant according to status of Hydro-ureter	36
Figure (4. 8) distribution of participant according to other findings	37
Figure (4. 8) distribution of participant according to type of stone	37

List of Abbreviations

BMI	Body Mass Index
BUN	Blood Urea Nitrogen
CT	Computerized Tomography
DMS	Data Measurement System
ED	Emergency Department
GE	General Electric
HIV	human immunodeficiency virus
HU	Hounsfield units
IVP	intravenous pyelogram
IVU	intravenous urogram
KUB	kidneys, ureters, and bladder
Max	Maximum
MDCT	Multi-detector computed tomography
MHU	MEGA HEAT Unit
Min	Minimum
MRI	Magnetic resonance imaging
NCCT	Non-Contrast Computed Tomography
PACS	picture archiving and communication system
PH	power of hydrogen
PUJ	Pelvic ureteric junction
SD	Standard Deviation
SFOV	Scan Field Of View
SPSS	Statistical Package for the Social Sciences
US	Ultrasound
VUJ	Vesico Ureteric Junction

List of Contents

Table	Page No
الاية	I
Dedication	II
Acknowledgement	III
Abstract	IV
المستخلص	V
List of tables	VI
List of figures	VII
List of abbreviation	VIII
List of Contents	IX
CHARTER ONE	
Introduction	
1.1 Introduction	1
1.2 Problem of the study	2
1.3 Objectives of the study:	2
1.3.1 The general objective:	2
1.3.2 The specific objective	2
1.4 Significant of study:	3
1.5 Overview of the study	3
CHARTER TWO	
Literature Review	
2.1 Anatomy	4
2.1.1 Blood supply:	6
2.2 The Physiology	7
2.3 pathology of the renal stone:	8
2.3.2 Risk Factors	9
2.3.3 Signs and symptoms	9

2.3.5 Diagnosing Kidney Stones	10
2.3.6 Treatment	11
2.4 Multi detector CT scan:	12
2.4.1 X-Ray Tube and Generator	12
2.4.2 Gantry	13
2.4.3 Data Rates and Data Transmission	13
2.4.4 Imaging Techniques	14
2.4.5 CT Interpretation	15
2.4.6 Pitfalls in Diagnosis	18
2.4.7 Indication Creep	19
2.5 Previous study:	20
CHAPTER THREE	
Materials & Methods	
3.1 Material:	26
Subject	26
3.1.1 Machine used	26
3.2. Method	27
3.2.1 Protocol:	27
3.2.2 Study area:	27
3.2.3 Study duration:	27
3.2.4 Inclusion criteria:	27
3.2.5 Statistical analysis:	27
3.2.6 Method o data collection	28
3.2.7Variables of the study:	28

CHAPTER FOUR	
Results	
4.1 Results	29-41
CHAPTER FIVE	
Discussion, Conclusion and Recommendations	
5.1 Discussion:	42
5.2 Conclusion	43
5.3 Recommendation:	44
References:	45
APPENDIX A	47
APPENDEX B	49

Chapter One

Introduction

1.1 Introduction

The urinary system is consisting of two kidneys, two ureters, urinary bladder, urethra and prostatic gland. Urinary tract obstruction is one of the commonest causes of renal hydronephrosis and renal failure. The early diagnosis of detects are very important to achieve the suitable treatment. There are several modalities which we use it in diagnosis of urinary tract diseases such as conventional x-ray, computerize tomography, magnetic resonance imaging, nuclear medicine and ultrasound. CT scan is frequently used to evaluate the internal structure of the body as stated by David Sutton et.al 1987. The CT scan of the kidneys for stones is a test that specifically looks for stones in the KUB (Caugberg et al., 2011).

This scan is frequently done in the emergency room for patient with sudden onset sharp side and acute pain and has blood in their urine. It is also ordered by outpatient doctors as well for similar symptoms. Spiral CT KUB is more accurate about 80% to detect small stone. Nowadays, many clinical centers chose to send cases with accident and emergency cases, urology for CT scan as their first option for easy diagnosis of the symptoms (Ren et al., 2019).

Single-slice and multislice spiral CT have forever changed the imaging of renal stone disease. A review of the techniques, findings, complications, and pitfalls involved is timely given that CT is now the imaging method of choice to detect renal stones and diagnose the complications of renal stone disease, acute flank pain is a common complaint of patients seeking emergency medical attention. Renal colic is the most common cause and is usually the major consideration for diagnostic imaging. Plain- film radiographs of the abdomen (often called KUB, for kidney-ureter-bladder) and excretory

urogram (also called IVP, for intravenous pyelo-gram) are the traditional imaging methods use diagnosis of renal stone disease and its complications. Plain radiographs have sensitivity for stones as low as 45%; however, with a specificity of only 77%. Non-contrast CT has been shown to be more effective than IVP in precisely identifying ureteral stones and is equally effective in determining the presence or absence of ureteral obstruction. Spiral CT has largely replaced plain radiographs and IVP. CT for stones requires no contrast and no patient preparation, and the study is routinely completed in less than 90 seconds (Bellin et al., 2004).

1.2 Problem of the study

Most of diagnostic modalities of urinary tract (conventional x-ray & ultrasound) don't give accurate diagnosis, or may lead to misdiagnosis when patient underwent conventional X-Ray for the kidneys, ureters and bladder due to various types of stone and its appearance.

1.3 Objectives of the study:

1.3.1 The general objective:

The general aim of this study was to evaluate the role of spiral computed tomography in the diagnosis of urinary tract stones.

1.3.2 The specific objectives:

- To correlate the number of the stones and its site to patient age.
- To correlate the stone site and the hydro-ureter,
- To identify the Hydronephrosis and obstructive changes.
- To identify the stone density
- To identify type of stone according to Hounsfield unit

1.4 Significant of study:

The study will provide rich information about CT KUB in detecting renal stones.

1.5 Overview of the study:

This study was consist of five chapters, chapter one was an introduction introduce briefly this thesis and contained (general introduction about the renal stone, problem of study also contains general and specific objectives, significant of the study and overview of the study). Chapter two was literature review about role of MDCT scanner in diagnosis of urinary tract stones, and other modalities used. Chapter three was describe the methodology (material, method) used in this study. Chapter four was included result of presentation of final finding of study; chapter five included discussion, conclusion and recommendation for future scope in addition to references and appendices.

Charter Two

Literature Review

2.1 Anatomy

The urinary system consists of two kidneys, two ureters, a urinary bladder, and a urethra. The kidneys are retroperitoneal structures of the abdomen, having migrated upward from the pelvis during development. They are maintained in their normal position by intra-abdominal pressure and by their connections with the perirenal fat and renal fascia (Ellis and Mahadevan, 2013).

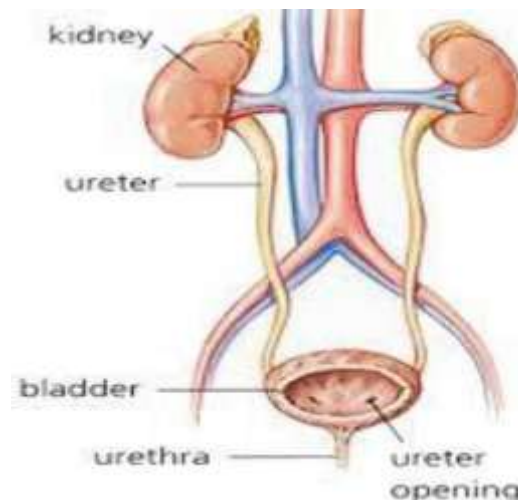


Figure (2.1) Showed the structure and component of renal system (Ellis and Mahadevan, 2013)

The kidney is bean-shaped with a superior and inferior pole. The midportion of the kidney is often called the mid-pole. In adults, each kidney is normally 10-12 cm in length, 3-5 cm in width and weighs 150-260 g. The left kidney is usually slightly larger than the right. The kidney has a fibrous capsule, which is surrounded by para-renal fat. The kidney itself can be divided into renal parenchyma, consisting of renal cortex and medulla, and the renal sinus containing renal pelvis, calyces, renal vessels, nerves, lymphatics and perirenal fat. The renal parenchyma has two layers: cortex and medulla. The renal cortex lies peripherally under the capsule while the renal medulla

consists of 10-14 renal pyramids, which are separated from each other by an extension of renal cortex called renal columns (Leslie and Sharma, 2019).

Urine is produced in the renal lobes, which consists of the renal pyramid with associated overlying renal cortex and adjacent renal columns. Each renal lobe drains at a papilla into a minor calyx, four or five of these unite to form a major calyx. Each kidney normally has two or three major calyces, which unite to form the renal pelvis. The renal hilum is the entry to the renal sinus and lies vertically at the anteromedial aspect of the kidney. It contains the renal vessels and nerves, fat and the renal pelvis, which typically emerges posterior to the renal vessels, with the renal vein being anterior to the renal artery (Leslie and Sharma, 2019).

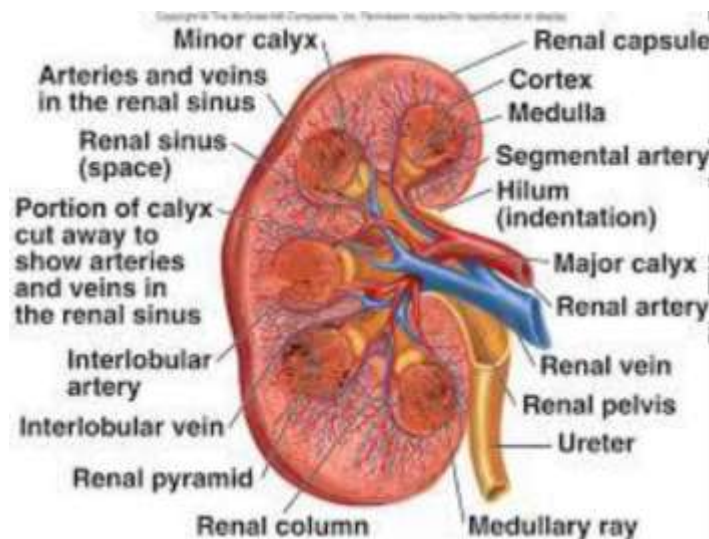


Figure (2.2) Showed the internal anatomical structure of the pelvicalceal system in addition to its nerve and blood supply (Leslie and Sharma, 2019)

The nephron of the kidney is made up of two major parts; the renal corpuscle and the tubules. These are then both sub-divided into various parts and overall it is this structure which allows the kidney to filter the blood and then alter the composition of this filtrate to ensure that waste products are excreted and useful compounds preserved. Renal corpuscle can be subdivided into the

glomerulus and the Bowman's capsule. The tubules are split into the proximal tubule, the loop of Henley, the distal tubule and the collecting ducts (Lauder et al., 2018).

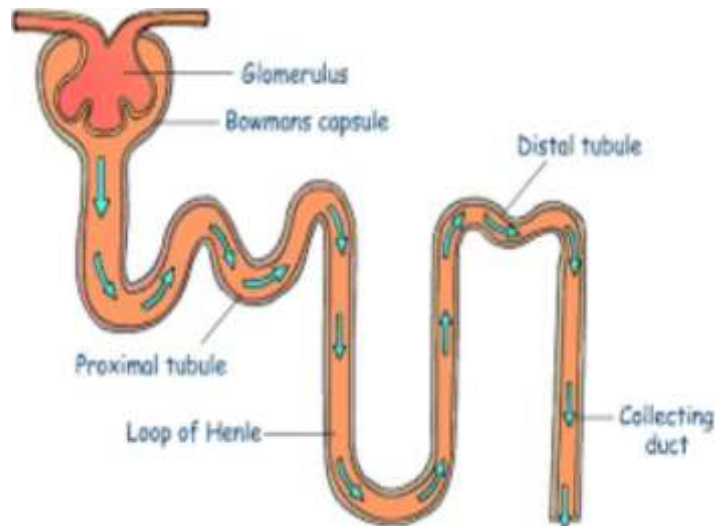


Figure (2. 3) Showed the internal structure of kidney's functional unit

2.1.1 Blood supply:

Blood reaches the kidneys through the renal arteries, which are short and come directly from the abdominal aorta. It divided into several inter-lobar arteries and give rise to the actuatearteries, which cross the border between the cortex and the medulla of the kidney. From the actuate arteries many branches radiate into the renal cortex; the inter-lobar arteries, the afferent arterioles arise at right angle from the interlobular arteries and end in the glomeruli (Lauder et al., 2018).

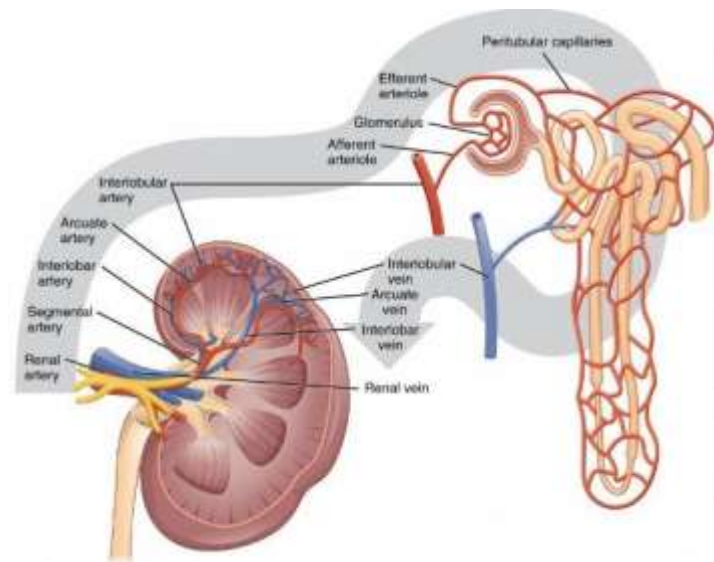


Figure (2. 4) Demonstrate the and blood pathway from and into the kidney (Lauder et al., 2018)

2.2 The Physiology

The kidneys play a major role in the control of the constancy of the internal environment. The blood flowing in kidneys is first filtered is call glomerular filtration so that the all blood constituents, except blood cell and plasma protein, go into the microtubular system. In these tubules, modifications of the filtrate take so that useful substances, including most of the filtered water, are quickly reabsorbed back into the blood. Unwanted substances that escape filtration are actively secreted into the lumen. The final concentration of electrolytes and other constituents of urine are adjusted according to the requirements of the regulation of the extracellular fluid composition. Glomerular filtration, tubular reabsorption and tubular secretion are rightly described as renal mechanisms that allow the kidney to undertake its various homoeostatic functions. Several hormones act on the kidney to enable it to adjust the final composition of urine in response to changes in the internal environment. The special features of renal circulation deserve an early description (Crabbs and McDorman, 2018).

These special characteristics are essential for the nephrons to perform their various functions. Function of the Urinary system will be summarized in; Regulation blood volume and pressure, regulating plasma concentration of sodium, potassium , chloride and other ions, stabilizing blood PH, conserving nutrients, and Detoxifying poisons with the liver (Crabbs and McDorman, 2018).

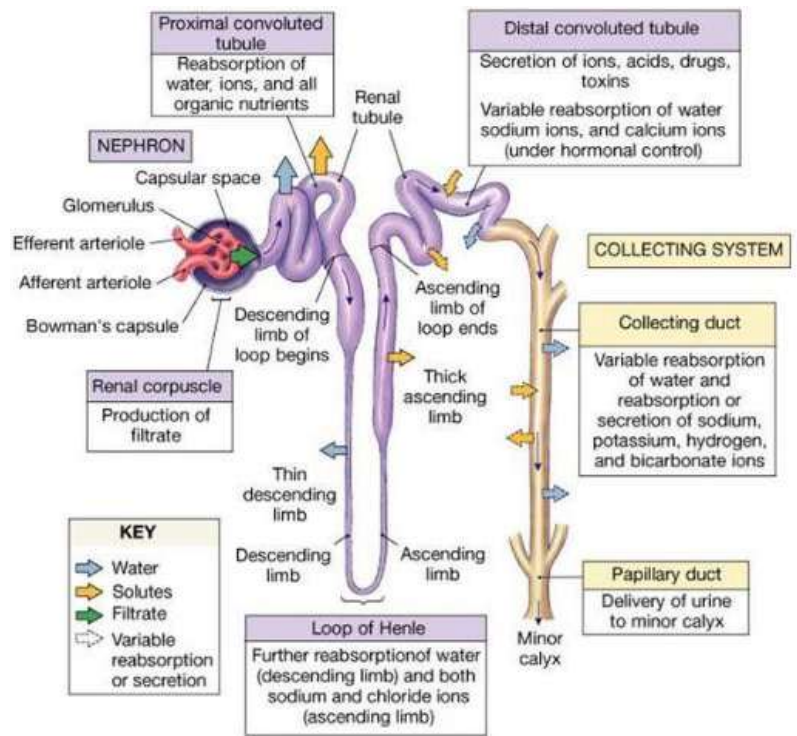


Figure (2. 5) Demonstrate the renal structure with its specific function (Crabbs and McDorman, 2018)

2.3 Pathology of the renal stone:

2.3.1 Types

Not all kidney stones are made up of the same crystals. The different types of kidney stones include: Calcium; Calcium stones are the most common. They can be made of calcium oxalate (most common), phosphate, or maleate. Vitamin C and spinach contain oxalate. Calcium-based kidney stones are most commonly seen in young men between the ages of 20 and 30, Uric Acid,

This type of kidney stone is more common in men than in women. They can occur in people with gout or those going through chemotherapy, Struvite, This type of stone are found mostly in women with urinary tract infection. These stones can be quite large and cause urinary obstruction. Cystine; rare type occur in both men and women who have the genetic disorder cystinuria. And other types of stone such as medications like triamterene and acyclovir also can cause stones (Curhan, 2007).

2.3.2 Risk Factors

The greatest risk factor for developing kidney stones is making less than one liter of urine per day. This why they are frequently seen in premature infants, who tend to have kidney problems. However, kidney stones are most likely to occur between the ages of 20 and 40. Other risk factors include: ethnicity (Caucasians are more likely to have kidney stones than African-Americans), sex (although kidney stones are most often seen in men, the incidence in women is increasing), past history of kidney stones (once someone has kidney stones, the likelihood of having another episode increases), family history of kidney stones, dehydration (dehydration causes decreased urine flow, which increases risk significantly), obesity, high- protein, salt, or glucose diet, gastric bypass surgery, inflammatory bowel diseases (which can cause increase calcium absorption) and other medical conditions (hyperparathyroidism can cause increase absorption of calcium and phosphorus; renal tubular acidosis can also be a risk factor for kidney stones (Curhan, 2007).

2.3.3 Signs and symptoms

Kidney stones are known to cause severe pain. Symptoms of kidney stones may not occur until the stone begins to move down the ureters. The severe pain is called renal colic. Pain may be located on one side of the back or abdomen. In men, pain may radiate to the groin area. The pain of renal colic

comes and goes, but is quite intense. People with renal colic tend to be restless. Other symptoms that can be present are: blood in the urine, vomiting, nausea, discolored or foulsmelling urine, chills, fevers (Rassweiler et al., 2000).

2.3.4 Complication

Stones don't always stay in the kidney. Sometimes, they pass from the kidney into the ureters. Ureters are small and delicate, and the stones may be too large to pass smoothly down the ureter to the bladder. Passage of stones down the ureter can cause spasms and irritation of the ureters as they pass, which causes blood to appear in the urine. Sometimes stones block the flow of urine. This is called a urinary obstruction. Urinary obstructions can lead to kidney infection (pyelonephritis) and kidney damage (Rassweiler et al., 2000).

2.3.5 Diagnosing Kidney Stones

Diagnosis of kidney stones requires a complete health history assessment and a physical exam. Other tests include: blood tests for calcium, phosphorus, uric acid and electrolytes, blood urea nitrogen (BUN) and creatinine to assess kidney functioning, urinalysis to check for crystals, bacteria, blood, and white cells and examination of passed stones to determine type. The following tests can rule out obstruction: abdominal X-rays, intravenous pyelogram (IVP), retrograde pyelogram, ultrasound of the kidney, MRI of the abdomen and kidneys and abdominal CT scan (Evan et al., 2007).

2.3.6 Treatment:

Treatment is tailored according to the type of stone. Urine can be strained and stones can be collected for evaluation. Drinking six to eight glasses of water a day increases urine flow. People who are dehydrated or have severe nausea and vomiting may need intravenous fluids. Other treatment options include: **Medication**; Pain relief may require narcotic medications. The presence of infection requires treatment with antibiotics. Other medications include: allopurinol for uric acid stones, diuretics, sodium bicarbonate or sodium citrate and phosphorus solutions (Evan et al., 2007).

Lithotripsy; Extracorporeal shock wave lithotripsy uses sound waves to break up large stones so they can more easily pass down the ureters into your bladder. This procedure can be uncomfortable and may require light anesthesia. It can cause bruising on the abdomen and back and bleeding around the kidney and nearby organs. Tunnel Surgery (Percutaneous Nephrolithotomy); Stones are removed through a small incision in your back and may be needed when: the stone causes (Takazawa et al., 2012). Obstruction and infection or is damaging the kidneys, the stone has grown too large to pass and pain cannot be controlled. And Ureteroscopy; when a stone is stuck in the ureter or bladder, your doctor may use an instrument called an ureteroscope to remove it. A small wire with a camera attached is inserted into the urethra and passed into the bladder. A small cage is used to snag the stone and remove it. The stone is then sent to the laboratory for analysis (Robertson, 2003).

2.4 Multi detector CT scan:

We use multi-detector CT scanning technology to see areas inside the body with micro-level detail. The multi-detector CT scanner allows us to obtain multiple slices in a single rotation, resulting in images that are of high quality, detail and clarity. Using this technology, we can also acquire data with great speed, so patients spend less time being scanned. In addition, the increased width of the scanning space of this tool makes for a more comfortable, less claustrophobic experience for patients (Bellin et al., 2004).

2.4.1 X-Ray Tube and Generator

State-of-the-art X-ray tube/generator combinations provide a peak power of 60– 100 kW, usually at various, user-selectable voltages, e.g., 80 kV, 100 kV, 120 kV and 140 kV. Different clinical applications require different X-ray spectra and hence different kV settings for optimum image quality and/or the best possible signal-to- noise ratio at the lowest dose. In a conventional tube design, an anode plate of typically 160–220-mm diameter rotates in a vacuum housing. The heat storage capacity of anode plate and tube housing— measured in Mega Heat Units (MHU)— determines the performance level: the bigger the anode plate is, the larger the heat storage capacity, and the more scan-seconds can be delivered until the anode plate reaches its temperature limit. A state-of-the-art X-ray tube has a heat storage capacity of typically 5 to 9 MHU, realized by thick graphite layers attached to the backside of the anode plate. An alternative design is the rotating envelope tube (STRATON, Siemens, Forchheim, Germany, Schardt et al. 2004). The anode plate constitutes an outer wall of the rotating tube housing; it is therefore in direct contact with the cooling oil and can be efficiently cooled via thermal conduction. This way, a very high heat dissipation rate of 5 MHU/min is achieved, eliminating the need for heat storage in the anode, which consequently has a heat storage capacity close to zero. Thanks to the

fast anode cooling, rotating envelope tubes can perform high power scans in rapid succession. Due to the central rotating cathode, permanent electromagnetic deflection of the electron beam is needed to position and shape the focal spot on the anode. The electro-magnetic deflection is also used for the double z-sampling technology of a 64-slice CT system (Ulzheimer and Flohr, 2009).

2.4.2 Gantry

Third-generation CT scanners employ the so-called “rotate/rotate” geometry, in which both the X-ray tube and detector are mounted onto a rotating gantry and rotate around the patient (Fig. 1.2). In a MDCT system, the detector comprises several rows of 700 and more detector elements that cover a scan field of view (SFOV) of usually 50 cm. The X-ray attenuation of the object is measured by the individual detector elements. All measurement values acquired at the same angular position of the measurement system form a “projection” or “view.” Typically, 1,000 projections are measured during each 360° rotation. The key requirement for the mechanical design of the gantry is the stability of both focal spot and detector position during rotation, in particular with regard to the rapidly increasing rotational speeds of modern CT systems (from 0.75 s in 1994 to 0.30 s in 2007). Hence, the mechanical support for the X-ray tube, tube collimator and data measurement system (DMS) has to be designed so as to withstand the high gravitational forces associated with fast gantry rotation (~17 g for 0.42 s rotation time, ~33 g for 0.33-s rotation time) (Ulzheimer and Flohr, 2009).

2.4.3 Data Rates and Data Transmission

With increasing numbers of detector rows and decreasing gantry rotation times, the data transmission systems of MDCT scanners must be capable of handling significant data rates: a four-slice CT system with 0.5-s rotation time roughly generates $1,000 \times 700 \times 4 \times 2$ bytes = 5.6 MB of data per rotation,

corresponding to 11.2 MB/s; a 16-slice CT scanner with the same rotation time generates 45 MB/s, and a 64- slice CT-system can produce up to 180–200 MB/s. This stream of data is a challenge for data transmission off the gantry and for real-time data processing in the subsequent image reconstruction systems. In modern CT systems, contactless transmission technology is generally used for data transfer, which is either laser transmission or electromagnetic transmission with a coupling between a rotating transmission ring antenna and a stationary receiving antenna. In the image reconstruction, computer images are reconstructed at rate of up to 40 images/s for a 512×512 matrix using special array processors (Ulzheimer et al., 2018).

2.4.4 Imaging Techniques

Also known as CT-KUB, renal stone CT is a spiral CT exam of the urinary tract that is used to diagnose the presence of urinary tract calculi and to detect acute urinary obstruction caused by stones. No oral or IVcontrast is administered (E.Brant, 2001).Spiral CT is markedly faster than conventional CT, allowing acquisition of a complete data set in a single breath-hold. This speed prevents the miss-registration of slice location that is characteristic of conventional CT.

Multislice spiral CT further decreases the time of acquisition, allowing for thinner slice collimation and retrospective reconstruction of thin slices to review problematic areas of interpretation. Data acquisition is continuous from the top of the kidneys through the base of the bladder (mid-liver [T-12] through symphysis pubis) using a maximum of 5-mmcollimation with table speed of 5 mm/sec. Slice collimation with multislice CT is usually 2.5 to 3 mm with table speed up to 5 mm/sec.Multislice technique allows slices as thin as 1mm to be obtained for problem-solving. Scanning can be performed using 2.5-mm collimation with fusion of images for viewing at 5-mm

thickness. The thinner slices can be viewed retrospectively without rescanning the patient. Thin slices allow identification of very small stones that may be overlooked with thicker slices. Turning the patient to a prone position permits differentiation of stones impacted at the ureterovesical junction from stones that have already passed into the bladder. When noncontrast renal stone CT is equivocal, intravenous contrast may be given to clarify the diagnosis. The pyelogram phase of contrast excretion is of most interest. Optimally, the ureters will be contrast-filled (Goldman, 2008).

An intravenous injection of 100 cc of 60% contrast is given; power injection is not needed. The renal stone protocol outlined above is repeated with a scan delay of three to five minutes after completion of contrast injection. This prolonged scan delay usually results in filling of both collecting systems and ureters. Thin slices (1 to 3-mm collimation) can be obtained through any area in question (E. Brant 2001).

2.4.5 CT Interpretation

CT may detect stones not evident on standard plain radiographs or IVP, It may also provide an alternative diagnosis for the patient's symptoms, including other urinary pathology, acute appendicitis, diverticulitis, pancreatitis, adnexal masses, or leaking aneurysms. While only about 85% of urinary stones are seen as calcific densities on plain films, CT detects nearly all calculi. Calcium oxalate and calcium phosphate stones are most common (73%) and typically have a CT attenuation of 800 to 1000 HU. Struvite, or magnesium aluminum phosphate, stones (15%) are seen with chronic infection. Their CT attenuation ranges from 300 to 900 HU. Uric acid stones (8%), which are usually radiolucent on plain film, have an attenuation of 150 to 500 HU. Cystine stones (1% to 4%) are moderately radiopaque because of their sulfur content. Calcium may be present in cystine stones, which have attenuation values of 200 to 880 HU, depending on calcium content. High

CT attenuation makes stones easy to differentiate from other urinary tract filling defects such as tumors, hematoma, fungus balls, or sloughed papilla. Virtually all stones, even those that are radiolucent on plain-film radiographs, are identified as highattenuation foci on CT images viewed on soft-tissue windows. Bell reported the mean attenuation of a series of calculi detected on CT as 305 HU with a range of 221 to 530 HU. Ureteral calculi are usually geometric or oval in shape and are seldom completely round. this feature is useful in differentiating stones from phleboliths. The positive predictive value of geometric shape in identifying a calculus has been reported as 100%. The single exception to the high-density appearance of stones on CT is crystalline stones in the urine related to use of protease inhibitors in the treatment of HIV disease. These stones are nonopaque on CT scans but may cause ureteral obstruction. Retrograde ureterogram, contrast- enhanced CT, or IVP demonstrates these stones as tiny radiolucent filling defects in the ureter (Bellin et al., 2004).

The burden of stones in the kidneys is easily determined by CT. Stones are seen in the region of the minor calices or medullary pyramids. The stone burden is defined as the number and size of stones present and is used to determine therapy, such as lithotripsy. The tips of the renal pyramids may show high attenuation, especially when the patient is dehydrated. This normal finding of “white pyramids” should not be interpreted as representing renal stones (Bellin et al., 2004).

Noncontrast spiral CT has a reported sensitivity of 94% to 98% and specificity of 96% to 98% for acute ureteral obstruction caused by an impacted stone. CT evaluation of acute ureteral obstruction caused by stones includes the following:

A stone is demonstrated in the ureter. The most common locations for stone impaction are at the uretero-pelvic junction, where the ureter crosses the

pelvic brim, and at the uretero-vesical junction. The ureter is followed on consecutive slices until a stone is identified. Scrolling on the CT monitor is the easiest way to follow the course of the ureter. Knowledge of the anatomy of the ureter and adjacent vessels is crucial for accurate interpretation, the size of the stone is measured and its location precisely reported. Stones smaller than 4 mm nearly always pass spontaneously; stones of 6 mm pass about half the time and those larger than 8 mm rarely pass spontaneously. Size and location are important factors in determining the treatment of stones that do not pass spontaneously. Stones larger than 5 mm and located in the proximal two-thirds of the ureter are more likely to require lithotripsy or endoscopic removal, to confirm a stone in the ureter, look for a tissue rim sign (present in about 76% of cases). The tissue rim sign describes a halo of soft tissue that surrounds stones in the ureter. The softtissuerim is the wall of the ureter. The tissue rim sign may be absent because of bloom effect artifact or a very thin ureteral wall, examination of the CT scout scan is useful for detecting stones and other abnormalities and should be included in every CT interpretation. If the stone is visible on the scout scan, plain radiographs can be used to monitor its passage. Calculi not visible on plain radiographs can be followed, when necessary, with unenhanced CT, Secondary findings of urinary obstruction are common but often subtle. Comparison to the opposite side is highly useful in differentiating preexisting findings from acute obstruction and the obstructed kidney may be enlarged and slightly decreased in CT density because of edema. The pelvicalyceal system is usually, but not always, mildly dilated (Bellin et al., 2004).

Dilated calyces are best seen at the poles as rounded fluidfilled structures that displace renal sinus fat. Comparison with the opposite kidney is always helpful. Profound dilatation of the collecting system is evidence of chronic, rather than acute, obstruction, Periureteral and perinephric fat stranding occurs secondary to edema produced by obstruction .The amount of edema

present correlates with the severity of obstruction. Unilateral absence of “white pyramids” on the affected side has been described as a subtle sign of obstruction; the ureter is mildly dilated to the level of the stone. Normal ureteral peristalsis produces transient focal areas of dilatation and narrowing. This must be differentiated from diffuse dilatation to the level of obstruction. The ureter below the obstructing calculus is not dilated.

Moderate or severe hydronephrosis suggests longer standing obstruction and should cause suspicion of other causes of ureteral obstruction, Focal perinephric fluid collections may occur secondary to forniceal rupture caused by obstruction and high urine output and axial plane CT images may be reformatted into coronal plane images that resemble IVP images in problematic cases and this procedure is time-consuming and seldom necessary for diagnosis. Some referring physicians may routinely request coronally reformatted images, however, because they resemble the trusted IVP (E. Brant et.al 2001).

2.4.6 Pitfalls in Diagnosis

No imaging test is perfect. A variety of pitfalls complicate interpretation of renal stone CT. An extrarenal pelvis may mimic pelviectasis. Peripelvic cysts can simulate hydronephrosis. Many patients, especially older ones, have preexisting stranding in the peripelvic fat. Comparison with the opposite side is critical to detection of asymmetric stranding, Phleboliths, which are calcifications that originate in thrombi within pelvic veins, commonly mimic stones. Most phleboliths are found in perivesical veins, in periprostatic veins in men, and in periuterine and perivaginal veins in women. They are occasionally seen in gonadal veins that parallel the course of the ureters, most phleboliths are round; they are seldom oval and are never geometric in shape, Visualization of a central lucency is highly characteristic of phleboliths but is less often evident on CT than on plain radiographs. A tail

sign represents a tail of noncalcified vein extending from the phlebolith. A tail sign has been reported with 21% to 65% of phleboliths. Phleboliths are lower density than most stones, with a mean attenuation value of 160 HU and a range of 80 to 278 HU.

The probability that a calcification represents a phlebolith is 0.03% when mean attenuation is 311 HU or more and atherosclerotic calcifications are occasionally mistaken for ureteral stones. Differentiation is made by carefully examining serial slices and determining if the calcification is in an artery or in the ureter also It is difficult to differentiate preexisting post-obstructive changes from acute obstruction.

When signs of ureteral obstruction are present but no stone is evident, consider a recently passed stone, pyelonephritis, stricture or tumor, or protease inhibitor treatment-related stone, Stones passed from the ureter may be identified in the bladder or urethra or may not be seen, always look for evidence of nonurinary causes of flank pain. Unenhanced CT has been reported to be 94% accurate in the diagnosis of appendicitis. Adnexal masses are usually easily detected, and a subsequent contrast-enhanced CT scan may be needed in up to 20% of cases to provide an unequivocal diagnosis.

2.4.7 Indication Creep

The quickness and ease of obtaining non-contrast CT for renal stones has resulted in a broadening of indications by referring physicians, especially emergency department physicians. The result is many more studies that are negative for stones but positive for a wider range of other urinary and non-urinary abnormalities, Noncontrast CT has substantial limitations for the diagnosis of solid masses in the liver, pancreas, and kidneys, as well as for conditions such as visceral ischemia, infarction, and infection. Radiologists may wish to broaden their use of contrast- enhanced CT to follow a negative or equivocal renal stone CT (E. Brant et.al 2001).

2.5 Previous studies:

A study conducted by (Kluner et.al 2006) to evaluate the diagnostic yield of multislice CT using a radiation dose equivalent to that of conventional abdominal x-ray (KUB). One hundred forty-two patients were prospectively examined with ultrasound and a radically dose-reduced CT protocol. Number and size of calculi, presence of urinary obstruction, and alternative diagnoses were recorded and confirmed by stone removal/discharge or by clinical and imaging follow-up. The mean effective whole-body dose was 0.5mSv in men and 0.7 mSv in women. The sensitivity and specificity in detecting patients with calculi was 97% and 95% for CT and 67% and 90% for ultrasound. Urinary obstruction was similarly assessed, whereas CT identified significantly more alternative diagnoses than ultrasound ($P < 0.001$). With regard to published data for standard-dose CT, the CT protocol seems to be comparable in its diagnostic yield in assessing patients with calculi, and its radiation dose is equivalent to that of KUB. Nephrolithiasis is the most common urinary tract disorder. The purposes of this study were to identify the most common type of kidney stones in Lebanon and evaluate the life style and pharmacological measures followed by Lebanese patients who have kidney stones This descriptive study is a part of the clinical nutrition course at the School of Pharmacy in a Lebanese university. Each student had to contact 10 patients from different community pharmacies between October 2013 and May 2014. Inclusion criteria included adults with kidney stones aged above 18 and living in Lebanon for more than 10 years. A 20 minutes face-to-face interview using a questionnaire was conducted. Descriptive statistical analysis was done by a pharmacist specialized in epidemiology. 550 patients with self-reported stone disease were enrolled. Results showed that the most common stone type is oxalate (62.7%) and least is cysteine (5.3%). The most taken medications are non-steroidal anti-

inflammatory drugs (58.2%) and paracetamol (34.9%). Patients' dietary habits included increased fluid intake (76.9%), decreased salt (38.4%) and meat consumption (34.7%) and avoidance of oxalate containing food (35.6%). In conclusion changing nutritional habits is one of the most accessible and inexpensive intervention to reduce kidney stones' risk. Educational and counseling efforts should be implicated in the management of nephrolithiasis (Marwan Akel, School of Pharmacy, Lebanese International University, Museitbeh, Beirut, Lebanon.2016)

The most useful CT reformatting technique was curved planar reformatting of the ureters to determine whether a ureteral calculus was present. In this study, noncontrast helical CT was a rapid and accurate method for determining the presence of ureteral calculi causing renal colic. The reformatted views produced images similar in appearance to excretory urograms, aiding greatly in communicating with clinicians. Limitations on the technique include the time and equipment necessary for reformatting and the suboptimal quality of reformatted images when little retroperitoneal fat is present. Another study conducted by Eray et.al 2001, to assess the diagnostic value of urinalysis and plain films in patients with suspected renal colic presenting to an emergency department (ED). Over a 1-year period, 138 patients presented to the ED during the daytime with suspected renal colic, but for technical reasons the diagnostic modalities used in the study could be completed for only 99 patients, and 34 patients were lost to follow-up. A urinalysis; kidney, ureter, and bladder film; and spiral computed tomography (CT) were performed on each patient. The presence of urinary tract stones was determined by their definite presence on helical CT and/or passage of a stone on clinical follow-up (average follow-up = 3 months). A urinary stone was visualized on spiral CT or passed in the urine in 54 of the patients. Using helical CT findings or passage of a stone as the gold standard, plain radiography had a sensitivity of 69% and specificity of 82%. Urinalysis had

a sensitivity of 69% and specificity of 27%. The sensitivity increased to 89% if either test was positive, but the specificity remained low at 27%. The sensitivity and specificity of CT in the diagnosis of urinary stones was 91%.

Poletti et.al 2007, compared a low-dose abdominal CT protocol, delivering a dose of radiation close to the dose delivered by abdominal radiography, with standard-dose unenhanced CT in patients with suspected renal colic. One hundred twenty-five patients (87 men, 38 women; mean age, 45 years) who were admitted with suspected renal colic underwent both abdominal low-dose CT (30 mAs) and standard-dose CT (180 mAs). Low-dose CT and standard-dose CT were independently reviewed, in a delayed fashion, by two radiologists for the characterization of renal and ureteral calculi (location, size) and for indirect signs of renal colic (renal enlargement, pyeloureteral dilatation, periureteral or renal stranding). Results reported for low-dose CT, with regard to the patients' body mass indexes (BMIs), were compared with those obtained with standard-dose CT (reference standard). The presence of non-urinary tract-related disorders was also noted. In patients with a BMI < 30, low-dose CT achieved 96% sensitivity and 100% specificity for the detection of indirect signs of renal colic and a sensitivity of 95% and a specificity of 97% for detecting ureteral calculi. In patients with a BMI < 30, low-dose CT was 86% sensitive for detecting ureteral calculi < 3 mm and 100% sensitive for detecting calculi > 3 mm. Low-dose CT was 100% sensitive and specific for depicting non-urinary tract-related disorders ($n = 6$).

The accuracy of NCCT in estimating ureteral stone size compared with plain abdominal (KUB) films was assessed by (Appledorn et.al 2003). Forty-eight patients were identified who ureteral stones had seen on NCCT and KUB films performed on the same day. The number of consecutive images on which a ureteral stone was visible on NCCT was multiplied by the reconstruction interval of 5 mm to create a size estimate, which was

compared with the measurements of the same stone seen on the KUB film. They found that, the NCCT overestimated stone size by approximately 30% to 50% compared with KUB.

Ahmed S. Nasef et al APRIL 2015 , The Overall renal ESWL success rate was 93.33%. The ESWL success rate was significantly higher for stone ≤ 15 mm than larger stones (97.62% versus 83.33%; $p=0.042$). The lower calyceal stones showed a lower ESWL success rate than stones in other kidney locations (76.92% versus 97.87%; $p=0.029$). ESWL was effective in 47 of 48 (97.92%) cases with stone density < 1000 HU and only in 9 of 12 (75.00%) of those with stone density ≥ 1000 HU ($p=0.023$). The stones with density values ≥ 1000 HU needed more energy, shockwaves and ESWL sessions than stones with a density values < 1000 HU ($p<0.001$). The most common type of stone detected were calcium oxalate stone (29.63%), followed by uric acid stone and mixed uric acid + calcium oxalate + calcium phosphate stones (20.37% for each). Calcium oxalate had the highest density values (902.73 ± 425.23 HU) and uric acid stones had the lowest values (364.00 ± 115.17). No significant differences were observed in the ESWL rates regarding stone compositions.

Sourtzis et.al 1999, was aimed to compare unenhanced helical CT and excretory urography in the assessment of patients with renal colic. Fiftythree of 70 consecutive patients with acute signs of renal colic were prospectively examined with unenhanced helical CT, which was followed immediately by excretory urography. Two radiologists who were unaware of the findings independently interpreted these examinations to determine the presence or absence of ureteral obstruction. On all CT scans that had positive findings for ureteral stones or obstruction, they looked for secondary signs of obstruction (perinephric or periureteral fat stranding, ureteral wall edema, ureteral dilatation, and blurring of renal sinus fat).A stone was recovered in

45 of the 53 patients, nine before and 36 after imaging. The latter 36 patients had their stones identified on CT, whereas only 24 patients had their stones identified on excretory urography. Eight patients without stone disease had normal ureters on both CT and excretory urography. Of the 45 patients who had stone disease, 26 had ureteral dilatation on both CT and excretory urography, and 36 patients who recovered a stone after CT had secondary signs of obstruction. Of the nine patients who recovered a stone before CT, three had secondary signs of obstruction. Two patients had periureteral fat stranding, ureteral wall edema, and renal sinus fat blurring. One patient had only ureteral wall edema. Compared with excretory urography, unenhanced helical CT is better for identifying ureteral stones in patients with acute ureterolithiasis.

Secondary CT signs of obstruction, including renal sinus fat blurring, were frequently present even when the stone was eliminated before imaging.

M. Patlas et.al 2014, they aimed to compare the accuracy of non-contrast spiral CT with ultrasound (US) for the diagnosis of ureteral calculi in the evaluation of patients with acute flank pain. 62 consecutive patients with flank pain were examined with both CT and US over a period of 9 months.

All patients were prospectively defined as either positive or negative for ureterolithiasis, based on follow-up evaluation. 43 of the 62 patients were confirmed as having ureteral calculi based on stone recovery or urological interventions. US showed 93% sensitivity and 95% specificity in the diagnosis of ureterolithiasis; CT showed 91% and 95%, respectively. Pathology unrelated to urinary stone disease was demonstrated in six patients. Although both modalities were excellent for detecting ureteral stones, consideration of cost and radiation lead us to suggest that US be employed first and CT be reserved for when US is unavailable or nondiagnostic.

M .Kalorin et al 2008, they proposed that younger children are less likely to pass renal calculi spontaneously, and that children younger than 10 years are more likely to have an identifiable metabolic abnormality and subsequently a higher risk of recurrence. We report our clinical outcomes in children with urinary calculi, specifically examining these factors. He performed a retrospective review of all pediatric patients diagnosed with renal or ureteral calculi at our institution between 2000 and 2007. Of 150 patients evaluated and treated during this period 80 (86 stones) had sufficient follow-up data to be included. Patients were divided into 2 groups according to age, namely 10 years or younger and older than 10 years. There were 39 patients in the younger group and 41 patients in the older group. Their main result was; of the younger cohort stones were ureteral in 43% and renal in 57%. The opposite trend was seen in older patients, with 69% having ureteral and 31% having renal stones ($p = 0.02$). Mean stone size (greatest dimension) did not differ significantly between the older and younger groups (6.9 mm vs 5.5mm, $p = 0.17$). Overall stone passage rate was 34% for younger and 29% for older patients ($p = 0.65$). No significant mean size differences in passed stones existed between the groups (3.2 mm vs 2.5 mm, $p = 0.31$). Overall younger vs. older ureteral stone passage rate was 37% vs 41% ($p = 0.58$), and for renal stones it was 32% vs 0%. Stones recurred in 7 younger and older patients. Younger children were more likely to present with renal stones, while older children had more ureteral stones. Overall children 10 years old or younger are as likely to pass stones as older children. Renal stones are more likely to be successfully managed expectantly in younger children. Metabolic abnormalities and stone recurrences are observed at similar rates between younger and older children

Chapter Three

Materials and Method

3.1. Material:

The study was executed using multi-detector computed tomography scanner MDCT 16-Slice scanner: 16-slice 0.625mm collimation, table feed 10 mm/rotation, effective tube current 37 mAs at 120 kV. Pitch = 10/40 mm collimation = 0.25. Average scan time = 5 s, to scan the patient with flank pain problems with 16-slice, detector array, fan beam shape, CT monitor for controlling scanning and processing

Subject:

100 patients were enrolled in the study; they were scanned with MDCT.

3.1.1 Machine used

TOPSHIPA device 16 slice Multi detector ;contrast injector (MedraoToshiba-2ways) for flush contrast media to patient and K-PACS system for diagnosis images and reconstruction and volume rendered purposes in addition to the density data measurement and stone type estimations.



Figure (3. 1) CT scan machine show gantry and couch

3.2. Method

3.2.1 Protocol:

Patients were placed in the supine position; Patients were also instructed to breathe normal and to drink much more fluid before the examination and not to urinate in order to see the full bladder volume and to clearly visualize the associated pathology. For patient's preparation, patient instructed not to eat 24 hours before the examination time and a cretin light food was identified to the patient such as foods not having oily component also milk component in order to evacuate the large intestine from the fecal masses and the abdominal gases that may interfere with stone and affect the image quality, a 3-5 mm cuts was performed from the level just below the diaphragm to the symphysis pubic in order to visualize the kidneys, ureter, and bladder and its associated morbidity.

3.2.2 Study area:

This study was conducted at Kassala state, HALFA ALGADIDA, YASHFEEN MEDICAL HOSPITAL.

3.2.3 Study duration:

This study was carried out from December 2019 to July 2020

3.2.4. Inclusion criteria:

The study was include all patients with flank pain at age between (4-80 years), female or male.

3.2.5 Statistical analysis:

All data were presented as mean \pm SD values. Data were analyzed by an independent t-test and by correlation analysis with the use of the SPSS (IBM SPSS version 21 (A value of $P < 0.05$ was considered significant).

3.2.6 Method of data collection:

The data were collected on master data sheet from the report which include all parameters need for evaluations.

3.2.7. Variables of the study:

Patient gender, Age, History of disease and Sign and symptoms, site, side, number of stone and Hounsfield unit.

Chapter Four Results

4.1 Results:

Table (4. 1) Distribution of participant according to gender:

Gender	Frequency	Percent
Male	60	60.0
Female	40	40.0
Total	100	100.0

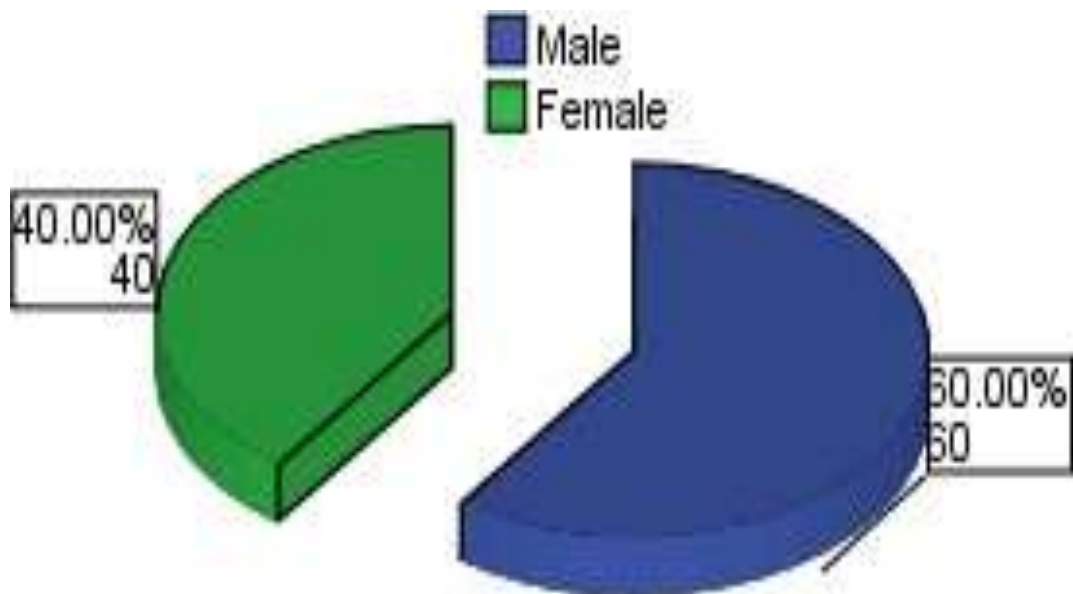


Figure (4. 1) Distribution of participant according to gender

Table (4. 2) Distribution of participant according to age

Age	Frequency	Percent
Less than 10 years	12	12.0
10-20 years	26	26.0
21-30 years	8	8.0
31-40 years	16	16.0
41-50 years	5	5.0
51-60 years	20	20.0
More than 60 years	13	13.0
Total	100	100.0

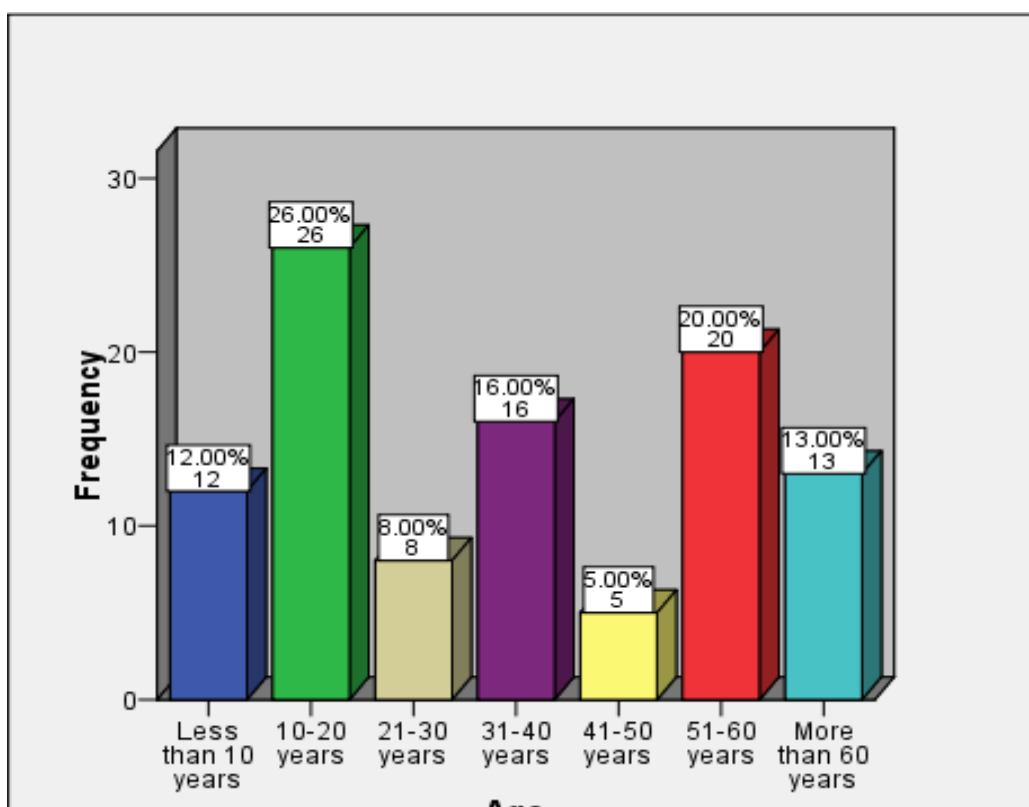


Figure (4. 2) Distribution of participant according to age

Table (4. 3) Distribution of participant according to Number of stones:

Number of stones	Frequency	Percent
1	73	73.0
2	18	18.0
3	6	6.0
4	1	1.0
5	2	2.0
Total	100	100.0

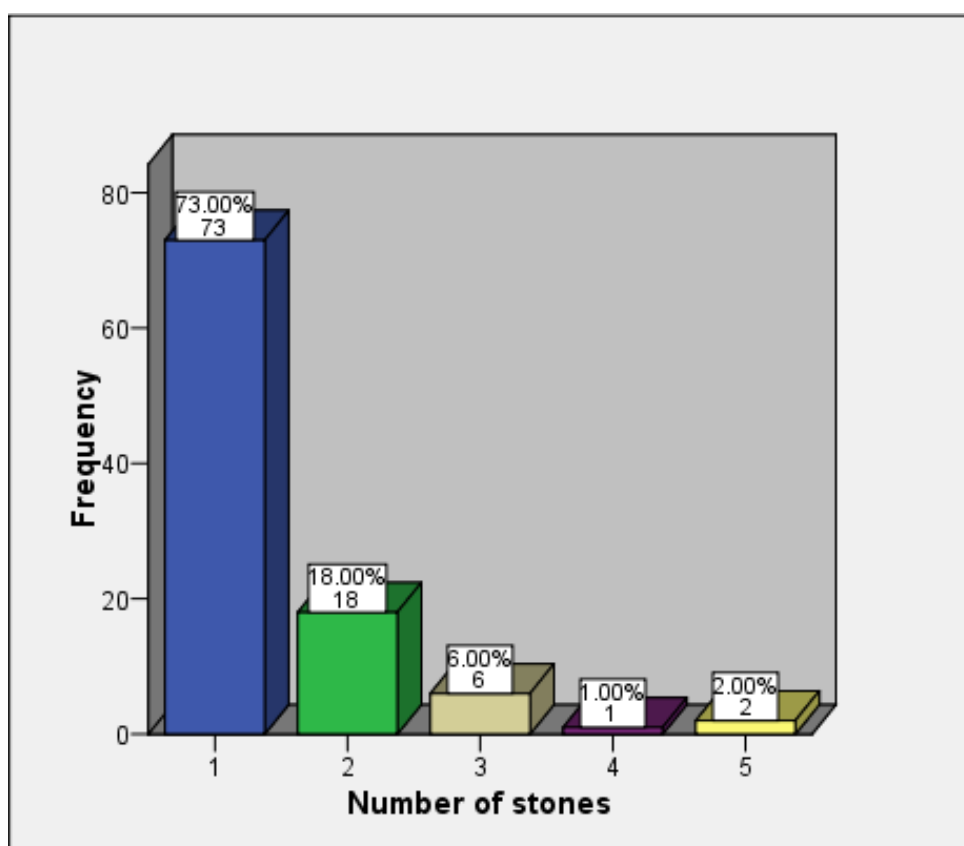


Figure (4. 3): distribution of participant according to No. of stones

Table (4. 4) Distribution of participant according to stone side

Stone site	Frequency	Percent
Right	43	43.0
Left	40	40.0
Both sites	17	17.0
Total	100	100.0

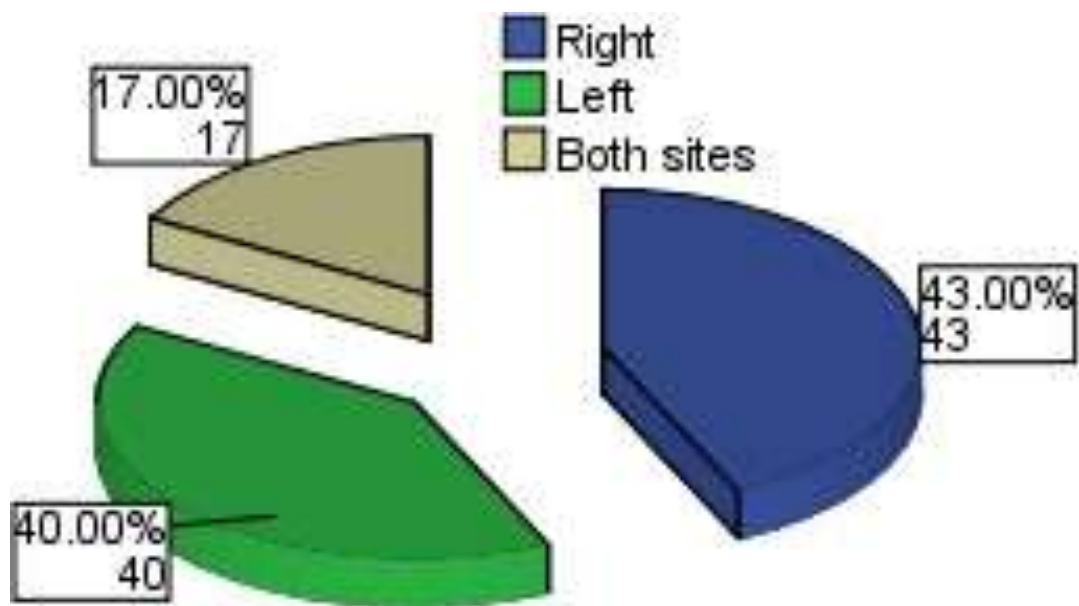


Figure (4. 4) distribution of participant according to stone site

Table (4. 5) Distribution of participant according to stone location:

Stone location	Frequency	Percent
Lower ureter	4	4.0
Lower calyces	21	21.0
Upper calyces	4	4.0
Pelvic of kidney	42	42.0
Upper ureter	2	2.0
Mid calyces	7	7.0
Mid ureter	10	10.0
Vesico uretric juncion	3	3.0
Lower ureter & lower calyces	5	5.0
Lower calyces & Pelvic	2	2.0
Total	100	100.0

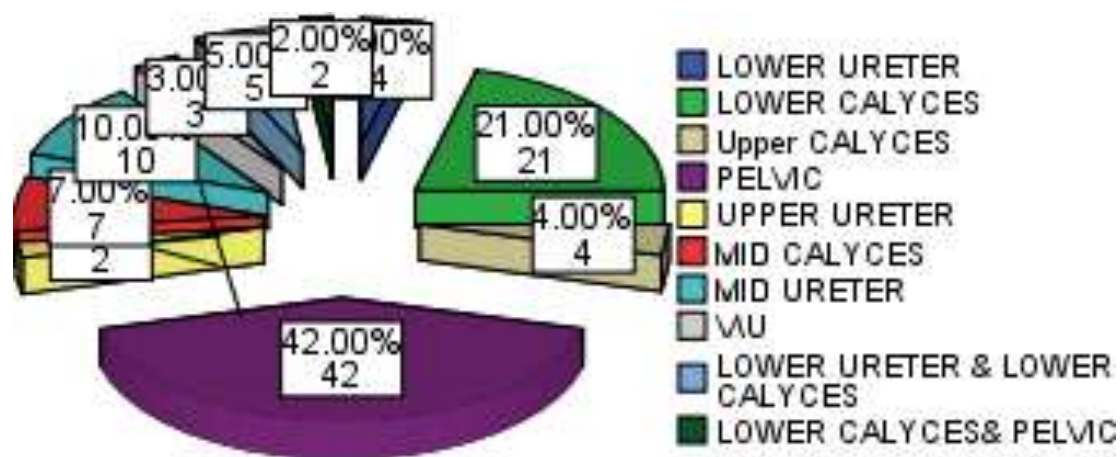


Figure (4. 5) Distribution of participant according to stone location

Table (4. 6) Distribution of participant according to status of Hydronephrosis:

Hydronephrosis	Frequency	Percent
No	34	34.0
Mild	28	28.0
Moderate	36	36.0
Sever	2	2.0
Total	100	100.
		0

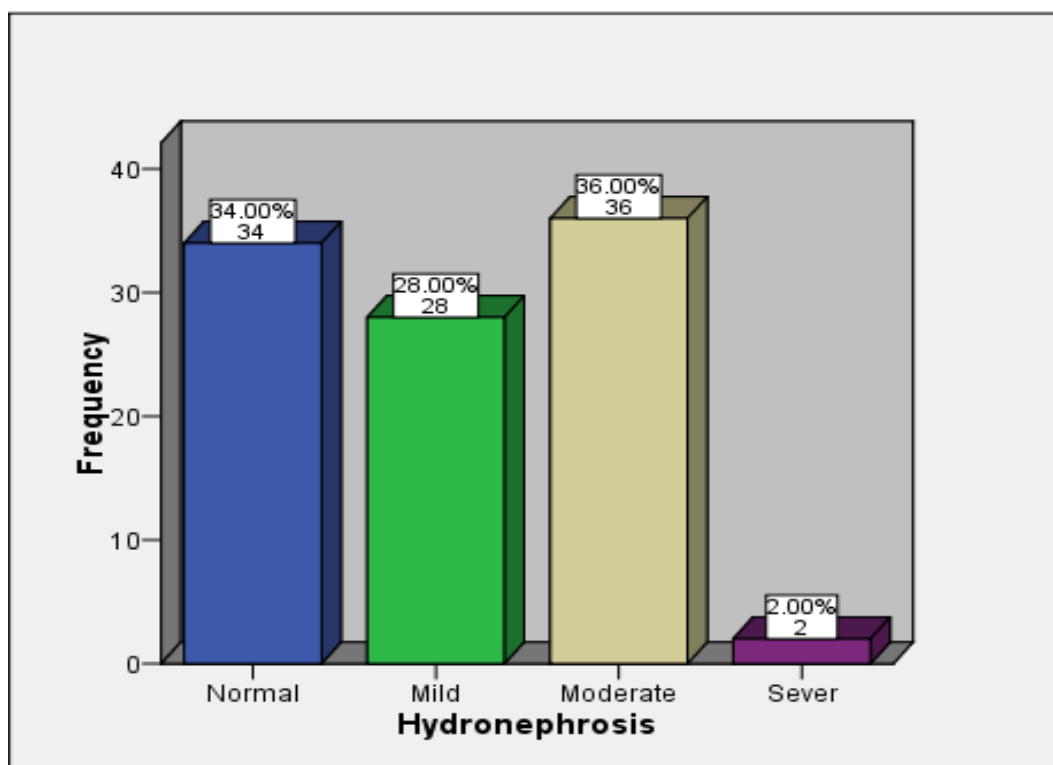


Figure (4. 6) Distribution of participant according to status of Hydronephrosis

Table (4. 7) Distribution of participant according to present of Hydroureter:

Hydro ureter	Frequency	Percent
YES	20	20.0
NO	80	80.0
Total	100	100.0

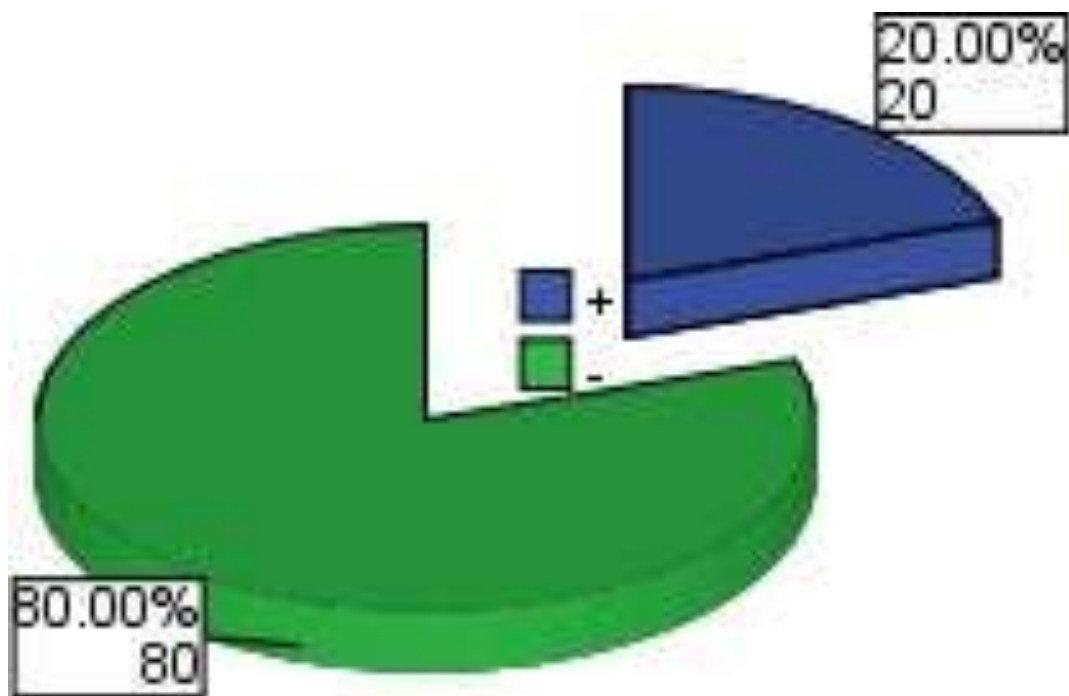


Figure (4. 7) Distribution of participant according to status of Hydro-ureter

Table (4. 8) Distribution of participant according to other findings:

Other findings	Frequency	Percent
Calyceal gravels	11	11.0
Pelvic uretric junction obstruction	11	11.0
Small kidneys	6	6.0
Cyst	6	6.0
Extra renals pelvic	4	4.0
Ascites	5	5.0
Gallbladder stones	4	4.0
Ectopia	2	2.0
No other findings	51	51.0
Total	100	100.0

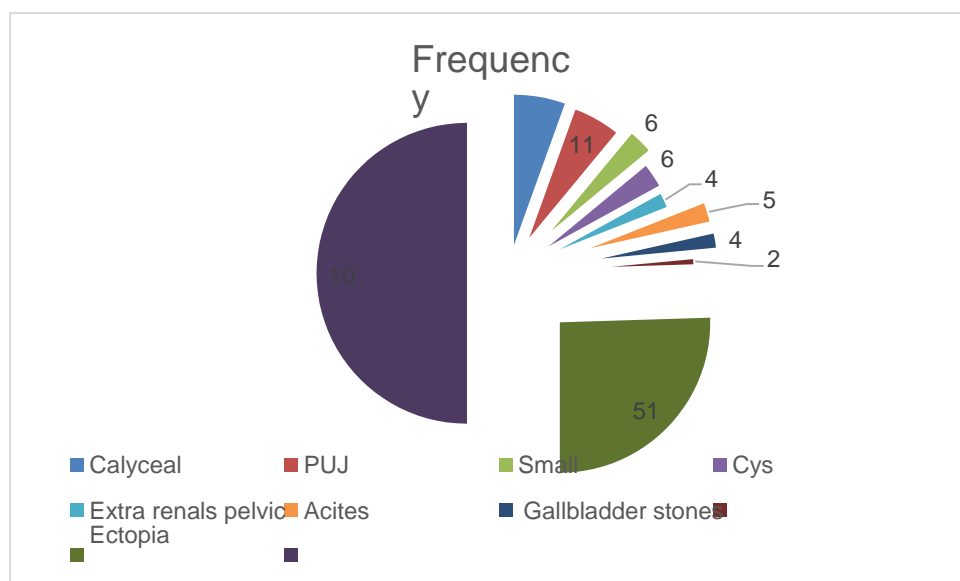


Figure (4. 8) Distribution of participant according to other findings

Table (4. 9) Distribution of participant according to the type of stone

Stone composition	Number of patient	percent
uric acid 200-450	6	6
stuvite 600-900	31	31
cystine 600-110	46	46
calcium phosphate 1200-1600	17	17
com and brushite 1700-2800	0	0
Total	100	100

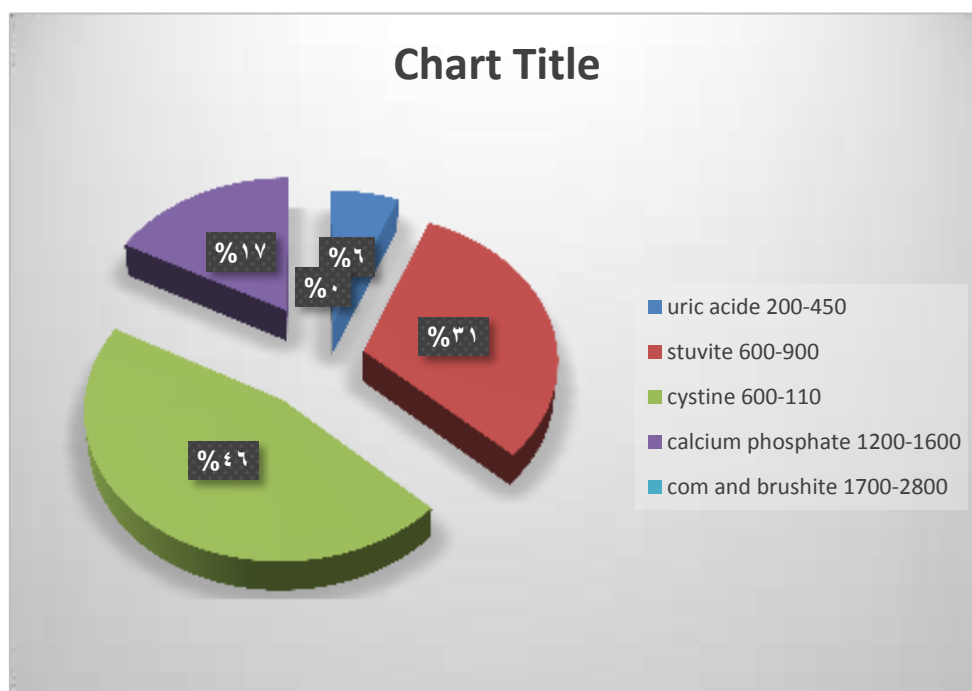


Figure (4. 9) Distribution of participant according to type of stone

Table (4. 10) Descriptive statistics for study variables:

	Minimum	Maximum	Mean	Std. Deviation
Density/HU	386.0	1594.0	946.492	244.5519
X-size/mm	3.0	33.5	10.333	6.7327
Y-size/mm	3.0	53.5	14.280	9.4816
Age/year	4	84	35.31	22.093

Table (4. 11) Chi-Square tests for association stone side and age:

Age		side			Total
		Right	Left	Both sides	
Less than 10 years	N	9	3	0	12
	%	75.0%	25.0%	.0%	100.0%
10-20 years	N	10	9	7	26
	%	38.5%	34.6%	26.9%	100.0%
21-30 years	N	7	0	1	8
	%	87.5%	.0%	12.5%	100.0%
31-40 years	N	6	9	1	16
	%	37.5%	56.2%	6.2%	100.0%
41-50 years	N	0	3	2	5
	%	.0%	60.0%	40.0%	100.0%
51-60 years	N	10	8	2	20
	%	50.0%	40.0%	10.0%	100.0%

					%
More than 60 years	N	1	8	4	13
	%	7.7%	61.5%	30.8%	100.0%
Chi-Square Tests					
	Value	df	Sig. (P-value)		
Likelihood Ratio	35.567	12	0.000		

Table (4. 12) Chi-Square tests for association No. of stones and age:

Age		Number of stones					Total
		1	2	3	4	5	
Less than 10 years	N	12	0	0	0	0	12
	%	100.0%	.0%	.0%	.0%	.0%	100.0%
10-20 years	N	17	5	2	0	2	26
	%	65.4%	19.2%	7.7%	.0%	7.7%	100.0%
21-30 years	N	8	0	0	0	0	8
	%	100.0%	.0%	.0%	.0%	.0%	100.0%
31-40 years	N	11	0	4	1	0	16
	%	68.8%	.0%	25.0%	6.2%	.0%	100.0%
41-50 years	N	2	3	0	0	0	5
	%	40.0%	60.0%	.0%	.0%	.0%	100.0%

51-60 years	N	18	2	0	0	0	20
	%	90.0%	10.0%	.0%	.0%	.0%	100.0%
More than 60 years	N	5	8	0	0	0	13
	%	38.5%	61.5%	.0%	.0%	.0%	100.0%
Chi-Square Tests							
		Value		df		Sig. (P-value)	
Likelihood Ratio		52.912		24		0.001	

Table (4. 13) Chi-Square tests for association stone site and Hydronephrosis:

		side			Total		
Hydro-nephrosis		Right	Left	Both sides			
No	N	18	10	6	34		
	%	41.9%	25.0%	35.3%	34.0%		
Mild	N	10	14	4	28		
	%	23.3%	35.0%	23.5%	28.0%		
Moderate	N	15	16	5	36		
	%	34.9%	40.0%	29.4%	36.0%		
Sever	N	0	0	2	2		
	%	.0%	.0%	11.8%	2.0%		
Chi-Square Tests							
		Value		df		Sig. (P-value)	
Likelihood Ratio		10.422		6		0.108	

Table (4. 14) Chi-Square tests for association stone site and Hydro-ureter

		Side			Total
Hydro-ureter		Right	Left	Both sides	
Yes	N	6	10	4	20
	%	14.0%	25.0%	23.5%	20.0%
No	N	37	30	13	80
	%	86.0%	75.0%	76.5%	80.0%
Chi-Square Tests					
		Value	df	Sig. (P-value)	
Likelihood Ratio		1.789	2	0.409	

Chapter Five

Discussion, conclusion and recommendations

5.1 Discussion:

A sample of (100), aged from 4 to 84 with mean 34 years (table 4.9), mostly (60%) male (table 4.1) was selected to evaluate the role multi detector computed tomography in the diagnosis of urinary tract stones.

The study showed that the majority (91%) of patients developed (1-2) stones (table 4.3), mostly on either right side (43%) or left side (40%) (Table 4.4), while the most stones located at pelvic of kidney (42%), lower calyces (21%) or mid ureter (10%) (Table 4.5), since most of patients developed mild (28%) or moderate (36%) Hydronephrosis (table 4.6) and mostly (80%) were no Hydro-ureter (table 4.7), whereas the most other findings were calyceal gravels (11%) or pelvic ureteric junction obstruction (11%) as shown in (Table 4.8). The study also showed that the most common type of stone according to the CT number was cysteine stone (46%), struvite (31%), calcium phosphate (17) (Table 4.8).

As for absolute values of attenuation for different types of stones, the results of our study with 127 human stones scanned in vitro confirm the results of (Mostafavi et al., 1998), who reported that stone composition can be identified using the attenuation value obtained from helical CT. this study showed that the stone density was (386- 1594) with mean 946.49 ± 244.55 (table 4.5) which appeared more dense. However, our overall results suggest that helical CT attenuation can be used to identify the probable composition of a urinary stone.

Regarding the size of the stone, the study showed that the size of the stone ranged (3-33.5) with mean 10.33 ± 6.73 in X-size and (3-53.5) with mean 14.28 ± 9.48 Y-size (table 4.9).

The study found that the stone site differ for the various age (P-value < 0.05) (table 4.10), as well as number of stones (P-value < 0.05) (table 4.11), while

Hydro- nephrosis does not depend on stone site (P-value >0.05) (table 4.12) nor Hydro- ureter (P-value > 0.05) (table 4.13).

5.2 Conclusion

The study was conducted to evaluate the role of multi detector computed tomography in the diagnosis of urinary tract stones. Among the patients most stones located at pelvic, lower calyces or mid ureter, with mostly mild or moderate Hydronephrosis and negative Hydro-ureter.

The study found that the CT number of the stone were (386-1594) with mean 946.49 ± 244.55 of HU, stone diameter (3-33.5) with mean 10.33 ± 6.73 X-size and (3-53.5) with mean 14.28 ± 9.48 Y-size.

The study found that the most common type of stone (according to the CT number) was cysteine stone followed by struvite stone.

The study found that the stone side differ for the various age groups, as well as number of stones (P-values < 0.05), neither Hydro-nephrosis nor Hydro-ureter do not depend on stone site (P-value > 0.05).

5.3. Recommendation:

- Prevention of urinary tract stones may include a combination of lifestyle changes and medications
- Lifestyle changes can be Drink water throughout the day, Eat fewer oxalate-rich foods if the patient tends to form calcium oxalate stones, choose a diet low in salt and animal protein and continue eating calcium-rich foods, but use caution with calcium supplements. Medications can control the amount of minerals and acid in the urine and may be helpful in people who form certain kinds of stones.
- The type of medication prescribes will depend on the kind of kidney stones.
- Farther study with large sample of patients.

References:

- BELLIN, M.-F., RENARD-PENNA, R., CONORT, P., BISSERY, A., MERIC, J.-B., DAUDON, M., MALLET, A., RICHARD, F. & GRENIER, P. 2004. Helical CT evaluation of the chemical composition of urinary tract calculi with a discriminant analysis of CT-attenuation values and density. *European radiology*, 14, 2134-2140.
- CAUBERG, E. C., NIO, C., DE LA ROSETTE, J. M., LAGUNA, M. P. & DE REIJKER, T. M. 2011. Computed tomography-urography for upper urinary tract imaging: is it required for all patients who present with hematuria? *J Endourol*, 25, 1733-1740.
- CRABBS, T. A. & MCDORMAN, K. S. 2018. Brief Synopsis: Review of Renal Tubule and Interstitial Anatomy and Physiology and Renal INHAND, SEND, and DIKI Nomenclature. *Toxicol Pathol*, 46, 920-924.
- CURHAN, G. C. 2007. Epidemiology of stone disease. *Urologic Clinics of North America*, 34, 287-293.
- ELLIS, H. & MAHADEVAN, V. 2013. *Clinical anatomy: applied anatomy for students and junior doctors*, John Wiley & Sons.
- EVAN, A. P., COE, F. L., LINGEMAN, J. E., SHAO, Y., SOMMER, A. J., BLEDSOE, S. B., ANDERSON, J. C. & WORCESTER, E. M. 2007. Mechanism of formation of human calcium oxalate renal stones on Randall's plaque. *The Anatomical Record: Advances in Integrative Anatomy and Evolutionary Biology: Advances in Integrative Anatomy and Evolutionary Biology*, 290, 1315-1323.
- GOLDMAN, L. W. 2008. Principles of CT: multislice CT. *Journal of nuclear medicine technology*, 36, 57-68.
- LAUDER, L., EWEN, S., TZAFRIRI, A. R., EDELMAN, E. R., LUSCHER, T. F., BLANKENSTIJN, P. J., DORR, O., SCHLAICH, M., SHARIF, F., VOSKUIL, M., ZELLER, T., UKENA, C., SCHELLER, B., BOHM, M. & MAHFOUD, F. 2018. Renal artery anatomy assessed by quantitative analysis of selective renal angiography in 1,000 patients with hypertension. *EuroIntervention*, 14, 121-128.
- LESLIE, S. W. & SHARMA, S. 2019. *Anatomy, Abdomen and Pelvis, Renal Artery*. StatPearls. Treasure Island (FL).
- MOSTAFAVI, M. R., ERNST, R. D. & SALTZMAN, B. 1998. Accurate determination of

chemical composition of urinary calculi by spiral computerized tomography. *The Journal of urology*, 159, 673-675.

RASSWEILER, J., RENNER, C. & EISENBERGER, F. 2000. The management of complex renal stones. *BJU international*, 86, 919-928.

REN, J. H., MA, N., WANG, S. Y., SUN, Y. J., ZHANG, Y. W., GUO, F. J., LI, Y. J., LI, T. H., AI, H., ZHANG, W. D., LI, P. & MA, W. H. 2019. Rationale and study design for one-stop assessment of renal artery stenosis and renal microvascular perfusion with contrast-enhanced ultrasound for patients with suspected renovascular hypertension. *Chin Med J (Engl)*, 132, 63-68.

ROBERTSON, W. G. Renal stones in the tropics. *Seminars in nephrology*, 2003. Elsevier, 77-87.

TAKAZAWA, R., KITAYAMA, S. & TSUJII, T. 2012. Successful outcome of flexible ureteroscopy with holmium laser lithotripsy for renal stones 2 cm or greater. *International Journal of Urology*, 19, 264-267.

ULZHEIMER, S., BONGERS, M. & FLOHR, T. 2018. Multi-slice CT: current technology and future developments. *Multislice CT*. Springer.

ULZHEIMER, S. & FLOHR, T. 2009. Multislice CT: current technology and future developments. *Multislice CT*. Springer.

APPENDIX A

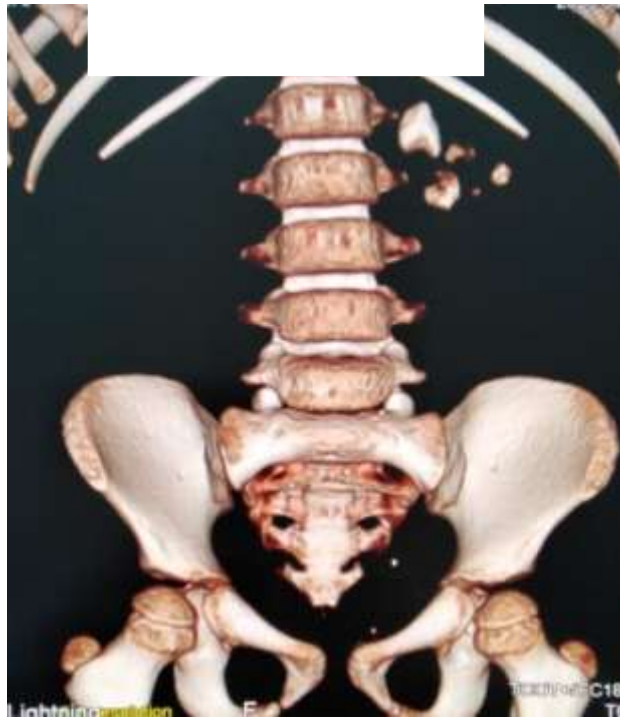


Image 1 Reconstructed CT KUB showed multiple stones in the Left Kidney



Image 2 axial CT showed stone in pelviureteric junction

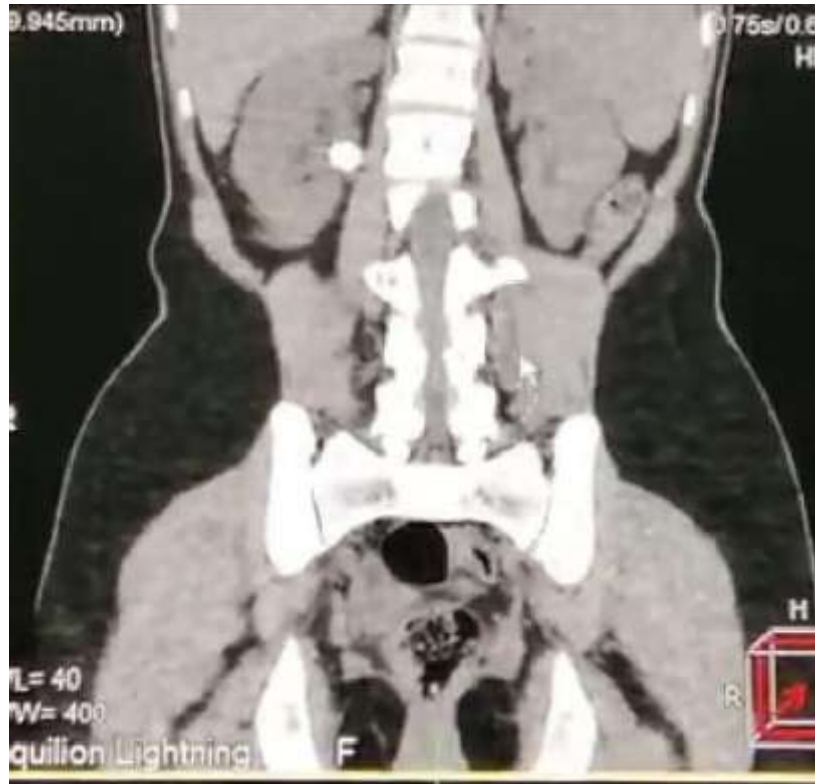


Image 3: coronal CT showed stone in the left kidney

